TAILORED MICRO-MESOPOROUS FERRIERITE CATALYSTS FOR CO_2 HYDROGENATION: INSIGHTS INTO STRUCTURAL MODIFICATION AND ACTIVITY

Nikola KOSTKOVÁ[1,2], Galina SÁDOVSKÁ[1,2], Radim PILAŘ[1], Eliška MIKYSKOVÁ[1], Darja SÁDOVSKÁ[1], Jaroslava MORÁVKOVÁ[1], Petr SAZAMA[1]

[1]*J. Heyrovský Institute of Physical Chemistry, Academy of Sciences of the Czech Republic, Prague, Czech Republic, EU, galina.sadovska@jh-inst.cas.cz*

[2]*University of Pardubice, Pardubice, Czech Republic, EU*

https://doi.org/10.37904/nanocon.2025.5208

Abstract

Hydrogenation of CO_2 to CH_4 over Ni-based catalysts is a promising route for renewable energy storage. This study investigates the role of micro-mesoporous ferrierite (FER) supports in stabilising Ni clusters and enhancing catalytic performance. Hierarchical ferrierite support was obtained by controlled desilication, resulting in mesopores approximately 4 nm in size and increased mesopore volume. Nickel (20 wt.%) was introduced by impregnation and subsequently reduced in H_2/N_2 mixture at 400 °C. Structural characterization (SEM, TEM, XRD, N_2 physisorption) revealed that Ni clusters in the desilicated sample (Ni-FER-desil.) were significantly smaller (~4 nm) and more uniformly dispersed within mesopores compared to larger (~17 nm) Ni particles on conventional FER in Ni-FER. In CO_2 methanation, Ni-FER-desil. exhibited superior CO_2 conversion and CH_4 selectivity, with catalytic productivity approximately 1.7 times higher than Ni-FER. These results demonstrate that desilication of ferrierite enhances Ni dispersion and provides a simple, scalable strategy to improve the performance of Ni-based methanation catalysts.

Keywords: CO_2 methanation, ferrierite, nickel catalysts, micro-mesoporous zeolites, dealumination, methane selectivity

1. INTRODUCTION

The methanation of carbon dioxide is a key process in carbon utilization, enabling the transformation of CO_2 into methane using hydrogen as a reducing agent. Known as the Sabatier reaction, this process is central to the Power-to-Gas (PtG) concept, which allows surplus renewable electricity to be stored as synthetic natural gas (SNG) [1-3]. In the context of a low-carbon economy and increasing availability of green hydrogen, CO_2 methanation offers a viable route for carbon recycling and long-term energy storage [3, 4].

From a catalytic perspective, the reaction is highly sensitive to the properties of both the active metal and the support. Nickel (Ni) is widely used due to its favourable cost-performance ratio [1]. Compared to noble metals such as Ru or Rh, Ni provides sufficient activity and selectivity, but is more prone to sintering and carbon deposition, leading to deactivation [2, 5]. Thus, achieving high activity requires finely dispersed Ni clusters anchored to a thermally stable and structurally optimized support.

Zeolites are attractive supports for Ni-based catalysts due to their high thermal stability, tuneable acidity, and well-defined pore architecture [6, 7]. However, their microporous nature often limits the dispersion of metal particles, as the pore size is typically smaller than the diameter of Ni clusters (2–20 nm). This spatial constraint can lead to aggregation on the external surface, reducing both activity and stability [8].

To overcome these limitations, a hierarchical micro-mesoporous zeolite has been employed, combining micropores with additional mesoporosity. Mesopores provide an enhanced external surface area and facilitate a better dispersion and accessibility of metal clusters [9]. Desilication in an alkaline medium is a widely used method to introduce intracrystalline mesoporosity, especially in zeolites with suitable Si/Al ratios. Studies have shown that such structural modifications improve the mass transport and utilization of active sites [10].

In this work, we investigate Ni catalysts supported on FER-type zeolites with either microporous (Ni-FER) or micro-mesoporous (Ni-FER-desil.) structures, both containing 20 wt.% Ni. The aim is to elucidate how hierarchical porosity affects Ni dispersion and catalytic performance in CO_2 methanation. Based on previous studies, we hypothesize that the mesoporous structure will enhance Ni dispersion and accessibility, leading to improved activity and selectivity.

2. EXPERIMENTAL

2.1 Preparation of Ni-FER catalysts

A commercial ferrierite zeolite (Si/Al molar ratio = 27, Zeolyst International) was used as the parent material. The micro-mesoporous ferrierite (denoted FER-desil.) was prepared by alkaline desilication in 0.2 M NaOH at 80 °C for 2 h under continuous stirring. After treatment, the solid was filtered, washed with deionized water until neutral pH, and dried at 80 °C overnight.

Nickel (20 wt.%) was introduced by impregnation using an aqueous solution of nickel(II) acetate tetrahydrate ($Ni(CH_3COO)_2 \cdot 4H_2O$). The impregnation was performed under vacuum using a rotary evaporator to ensure homogeneous metal distribution. This method was selected based on prior studies showing that solvent choice and impregnation conditions significantly influence Ni dispersion and particle size [8, 11]. The impregnated samples were dried at 80 °C overnight and calcined in air at 500 °C for 4 h. Prior to catalytic testing, the catalysts were reduced in a flow of H_2/N_2 (6 mL min^{-1} H_2, 114 mL min^{-1} N_2) at 400 °C for 1 h. The resulting samples are referred to as Ni-FER and Ni-FER-desil., respectively.

2.2 Characterization of Ni-FER catalysts

Textural and structural properties were characterized using N_2 physisorption, high-resolution transmission electron microscopy (HR-TEM), scanning electron microscopy (SEM), and X-ray diffraction (XRD). The N_2 adsorption–desorption isotherms were recorded at −196 °C after degassing the samples at 300 °C under vacuum for 4 h. The surface areas of the BET were calculated in the relative pressure range p/p_0 = 0.05–0.25, and the pore size distributions were derived from the adsorption branch using the BJH method. The morphology and dispersion of Ni clusters were observed by high-resolution transmission electron microscopy (HR-TEM) and scanning electron microscopy (SEM). HR-TEM images were acquired using a field-emission transmission electron microscope operating at 200 kV. XRD patterns were recorded using Cu Kα radiation (λ = 1.5406 Å) in the 2θ range of 5–80° at a scanning rate of 2° min^{-1}.

2.3 Catalytic activity measurements

Catalytic performance in CO_2 methanation was evaluated in a continuous-flow fixed-bed reactor at atmospheric pressure. Prior to reaction, each catalyst (10 mg, particle size 0.3–0.6 mm) was reduced in situ in a 5 vol.% H_2/95 vol.% He mixture at 400 °C for 30 min.

The feed gas consisted of CO_2 and H_2 in a 1:4 molar ratio, balanced with helium. The total gas hourly space velocity (GHSV) was maintained at 300,000 h^{-1}. Catalytic activity was tested in the temperature range of 200–400 °C. The reactor effluent was analysed online using a gas chromatograph equipped with thermal conductivity (TCD) and flame ionization (FID) detectors. CO_2 conversion, CH_4 selectivity and catalyst

productivity were calculated on the basis of carbon balances, assuming CH_4 and CO as the only carbon-containing products.

3. RESULTS AND DISCCUSSIONS

3.1 Structure of Ni catalysts

Figure 1 compares SEM and TEM images, XRD patterns, and N_2 adsorption–desorption isotherms of the parent and desilicated ferrierite zeolites. Microscopy confirms that the desilicated sample (FER-desil.) contains an additional network of mesopores with a sharp maximum of the pore size at 3.5 nm, while the parent FER retains its microporous structure Figure 1A). XRD patterns of both materials on Figure 1B show characteristic reflections of the FER framework, indicating that crystallinity is largely preserved after alkaline treatment. However, FER-desil. exhibits slightly broadened and less intense reflections, consistent with partial loss of long-range order, as commonly observed in desilicated zeolites [10, 12]. The N_2 isotherms further support the formation of hierarchical porosity. FER shows a Type I isotherm typical of microporous materials, while FER-desil. displays a combined Type I/IV profile with a pronounced hysteresis loop in the p/p_0 range of 0.45–0.90, characteristic of mesoporous structure [9, 13]. Textural data (**Table 1**) reveal that mesopore volume increased from 0.12 to 0.21 $cm^3\,g^{-1}$ after desilication, while the external surface area increased from 48 to 79 $m^2\,g^{-1}$. These changes confirm the successful introduction of intracrystalline mesoporosity, which enhances the mass transport and accessibility of active sites.

Table 1 Textural properties of the parent and desilicated ferrierite supports.

Sample	S ($m^2\,g^{-1}$)	S_{ext} ($m^2\,g^{-1}$)	V_{tot} ($cm^3\,g^{-1}$)	V_{micro} ($cm^3\,g^{-1}$)	V_{meso} ($cm^3\,g^{-1}$)
FER	351	48	0.24	0.12	0.12
FER−desil.	270	79	0.32	0.10	0.21

Structural analysis of the Ni catalysts is shown in **Figure 2**. HR-TEM analysis of reduced catalysts reveals significant differences in the size and distribution of Ni particles (**Figure 2A**). Ni-FER contains relatively large Ni clusters (~17 nm) located mainly on the external surface. In contrast, Ni-FER-desil. exhibits highly dispersed Ni nanoparticles (~4 nm) embedded within mesoporous regions. These findings are corroborated by XRD (**Figure 2B**), where Ni-FER shows sharp reflections for metallic Ni^0, while Ni-FER-desil. displays broader, less intense peaks, consistent with smaller crystallites.

Table 2 summarizes the size and dispersion of the Ni particles. The dispersion of Ni in Ni-FER-desil. (18.9%) is more than three times higher than in Ni-FER (5.8%), demonstrating the effectiveness of mesoporous architecture in stabilizing small Ni clusters. Similar enhancements have been reported for Ni catalysts supported on mesoporous alumina and zeolites [8, 11, 14]. The parameter describing the catalytic activity, referred to as catalyst productivity, was calculated at 400 °C based on the reaction rate determined for a zero-order reaction [15].

Table 2 Average Ni particle size and metal dispersion of Ni-FER and Ni-FER-desil. catalysts.

Catalyst	Si/Al	Ni (wt.%)	d_{Ni} (nm)	D (%)	Cat. productivity (mol $g_{cat}^{-1}\,s^{-1}$)
Ni-FER	27	20.1	17 ± 9	5.8	1.0×10^{-4}
Ni-FER-desil.	12.6	20.2	4 ± 2	18.9	1.7×10^{-4}

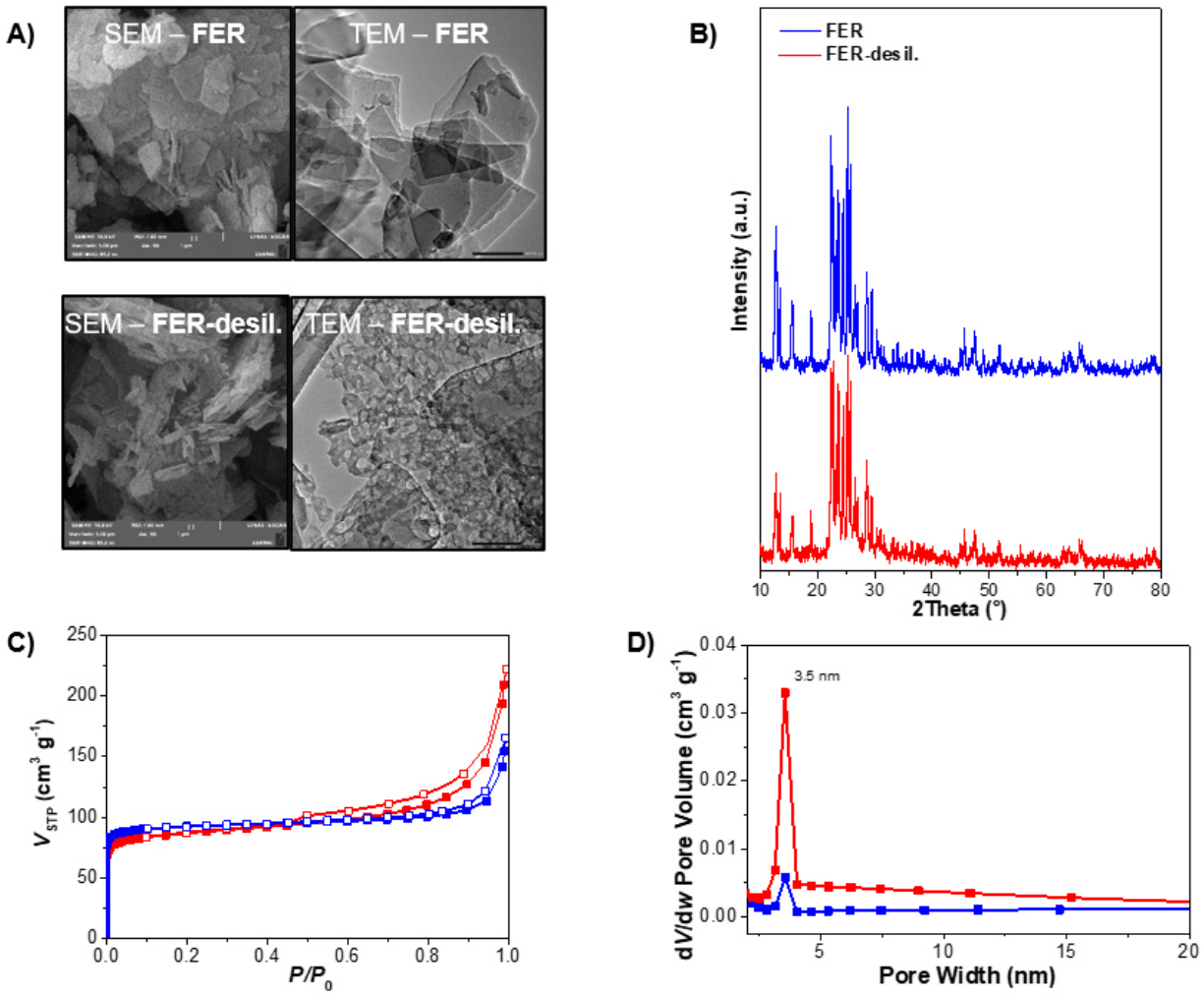

Figure 1 A) SEM and TEM images, B) XRD patterns, C-D) N_2 adsorption–desorption isotherms and D) pore volume of parent FER and desilicated FER zeolites.

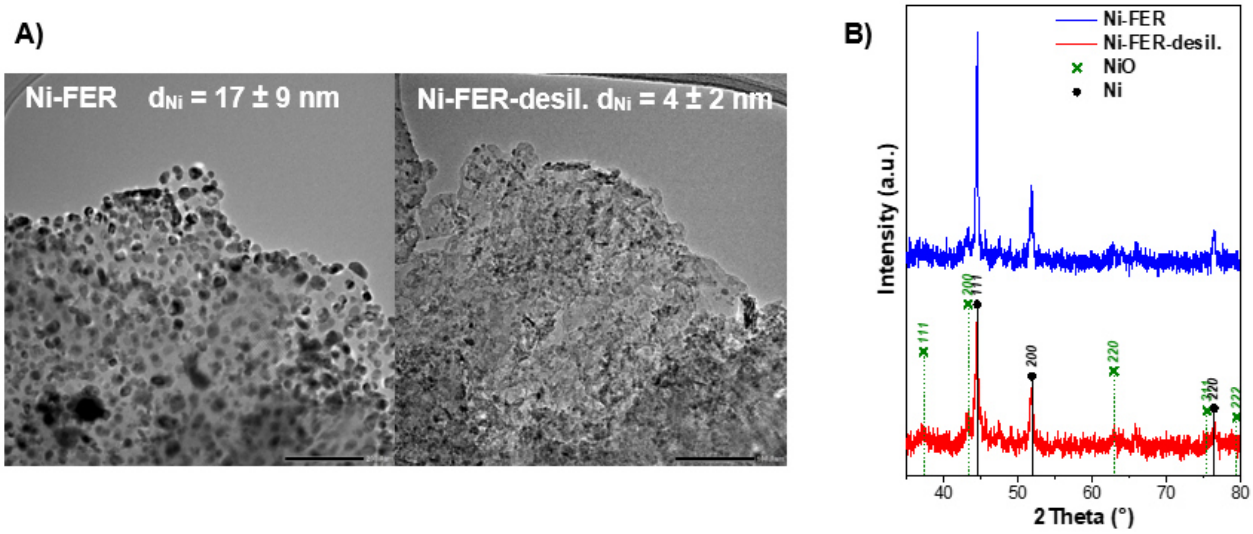

Figure 2 A) HR-TEM images of reduced Ni-FER and Ni-FER-desil. B) Powder XRD patterns of Ni-FER and Ni-FER-desil.

3.2 Catalytic activity in CO_2 methanation

CO_2 methanation can proceed through a direct hydrogenation pathway or through a two-step mechanism involving reverse water-gas shift (RWGS) followed by CO methanation [4]. The catalytic performance of Ni-FER and Ni-FER-desil was evaluated in the temperature range 200–400 °C. **Figure 3** shows the conversion of CO_2 and the selectivity of the product. The conversion of CO_2 is plotted as a function of reaction temperature, and the selectivity to CH_4 and CO is plotted as a function of CO_2 conversion. Both catalysts exhibit increasing conversion with temperature, while Ni-FER-desil. outperforms Ni-FER in the whole temperature range. At 400 °C, conversion of CO_2 reaches 23% for Ni-FER-desil., compared to 14% for Ni-FER. Consistently, the selectivity for CH_4 over Ni-FER-desil. slightly exceeds Ni-FER. The calculated productivity of Ni-FER-desil. is approximately 1.7 times higher than that of Ni-FER, confirming the catalytic advantage of Ni nanoparticles dispersed in the structure with hierarchical porosity.

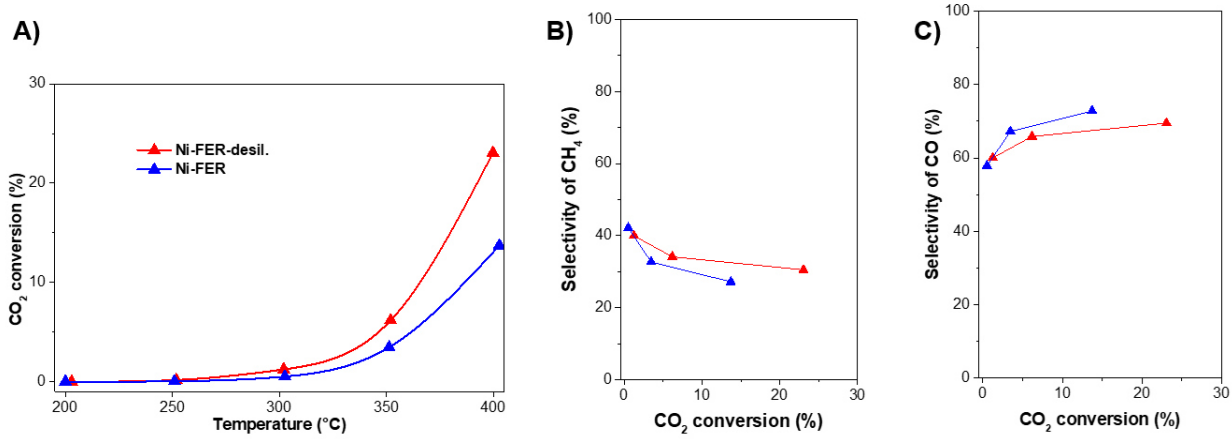

Figure 3 A) CO_2 conversion as a function of reaction temperature and product selectivity of Ni-FER and Ni-FER-desil. catalysts as a function of CO_2 conversion for B) CH_4 and C) CO.

The superior performance of Ni-FER-desil. can be ascribed to several interrelated factors. The incorporation of mesopores enhances the external surface area, facilitating more uniform Ni dispersion and improved accessibility of active sites for CO_2 and H_2 molecules. Smaller Ni particles exhibit a higher proportion of surface Ni^0 atoms, which are crucial for CO_2 activation and hydrogenation [2, 5]. Similar effects have been observed for Ni catalysts supported in mesoporous aluminosilicates [11, 14]. Bacariza et al. [8] demonstrated that reducing the size of Ni particles below 10 nm significantly improves the CH_4 formation rates due to stronger metal–support interactions. Thus, the superior activity of Ni-FER-desil. arises from its hierarchical micro-mesoporous architecture, which enables both optimal Ni dispersion and efficient mass transport, resulting in improved conversion and selectivity in CO_2 methanation. These findings are consistent with the broader literature, where hierarchical supports have been repeatedly shown to enhance activity, selectivity, and stability in CO_2 methanation systems [6, 7, 11].

4. CONCLUSIONS

Ni catalysts supported on ferrierite zeolites were synthesized and evaluated for CO_2 methanation. The catalyst based on desilicated ferrierite (Ni-FER-desil.) exhibited significantly enhanced performance compared to the conventional Ni-FER sample. Structural characterization confirmed that Ni-FER-desil. contains finely dispersed Ni clusters (~4 nm) located within secondary mesopores, while Ni-FER has larger agglomerates (~17 nm) predominantly on the external surface.

The improved Ni dispersion in Ni-FER-desil. resulted in higher CO_2 conversion and CH_4 selectivity throughout the tested temperature range, with catalyst productivity approximately 1.7 times greater than that of Ni-FER.

These findings demonstrate that the introduction of hierarchical micro-mesoporosity via controlled desilication effectively enhances Ni dispersion and catalytic efficiency without compromising the integrity of the zeolitic framework.

This strategy aligns with larger trends in catalyst design, where hierarchical supports such as desilicated zeolites [10, 12], ordered mesoporous alumina, and MOF-derived alumina have shown superior performance in CO_2 methanation. The Ni-FER-desil. system thus represents a robust and scalable platform for efficient CO_2 hydrogenation and related catalytic processes.

ACKNOWLEDGEMENTS

This work was supported by the Technology agency of the Czech Republic under project no. TS01030146 and by the Project OP JAK_Amulet, no. CZ.02.01.01/00/22_008/0004558, of the Ministry of Education, Youth and Sports, which is co-funded by the European Union. We also acknowledge the support and resources provided by the Research Infrastructure NanoEnviCz (Project No. LM2023066). N. K. acknowledges the Internal Grant Agency of the University of Pardubice under project No. SGS_2025_006.

REFERENCES

[1] RÖNSCH, S., SCHNEIDER, J., MATTHISCHKE, S., SCHLÜTER, M., GÖTZ, M., LEFEBVRE, J., PRABHAKARAN, P., BAJOHR, S. Review on methanation – From fundamentals to current projects. *Fuel*. 2016, vol. 166, pp. 276-96. Available from: https://doi.org/10.1016/j.fuel.2015.10.111

[2] YOUNAS, M., LOONG KONG, L., BASHIR, M.J.K., NADEEM, H., SHEHZAD, A., SETHUPATHI, S. Recent Advancements, Fundamental Challenges, and Opportunities in Catalytic Methanation of CO2. *Energy & Fuels*. 2016, vol. 30, no. 11, pp. 8815-31. Available from: https://doi.org/10.1021/acs.energyfuels.6b01723

[3] GÖTZ, M., LEFEBVRE, J., MÖRS, F., MCDANIEL KOCH, A., GRAF, F., BAJOHR, S., REIMERT, R., KOLB, T. Renewable Power-to-Gas: A technological and economic review. *Renewable Energy*. 2016, vol. 85, pp. 1371-90. Available from: https://doi.org/10.1016/j.renene.2015.07.066

[4] CHAMPON, I., BENGAOUER, A., CHAISE, A., THOMAS, S., ROGER, A.-C. Carbon dioxide methanation kinetic model on a commercial Ni/Al2O3 catalyst. *Journal of CO2 Utilization*. 2019, vol. 34, pp. 256-65. Available from: https://doi.org/10.1016/j.jcou.2019.05.030

[5] LV, C., XU, L., CHEN, M., CUI, Y., WEN, X., LI, Y., WU, C.-E., YANG, B., MIAO, Z., HU, X., SHOU, Q. Recent Progresses in Constructing the Highly Efficient Ni Based Catalysts With Advanced Low-Temperature Activity Toward CO2 Methanation. *Frontiers in Chemistry*. 2020, vol. 8, pp. Available from: https://doi.org/10.3389/fchem.2020.00269

[6] MACHADO-SILVA, R.B., DA COSTA-SERRA, J.F., CHICA, A. Enhancement of catalytic activity in CO2 methanation in Ni-based catalysts supported on delaminated ITQ-6 zeolite. *Journal of Catalysis*. 2024, vol. 436, pp. 115609. Available from: https://doi.org/10.1016/j.jcat.2024.115609

[7] YAN, P., PENG, H., WU, X., RABIEE, H., WENG, Y., KONAROVA, M., VOGRIN, J., ROZHKOVSKAYA, A., ZHU, Z. Impact of varied zeolite materials on nickel catalysts in CO2 methanation. *Journal of Catalysis*. 2024, vol. 432, pp. 115439. Available from: https://doi.org/10.1016/j.jcat.2024.115439

[8] BACARIZA, M.C., AMJAD, S., TEIXEIRA, P., LOPES, J.M., HENRIQUES, C. Boosting Ni Dispersion on Zeolite-Supported Catalysts for CO2 Methanation: The Influence of the Impregnation Solvent. *Energy & Fuels*. 2020, vol. 34, no. 11, pp. 14656-66. Available from: https://doi.org/10.1021/acs.energyfuels.0c02561

[9] SERRANO, D.P., ESCOLA, J.M., PIZARRO, P. Synthesis strategies in the search for hierarchical zeolites. *Chemical Society Reviews*. 2013, vol. 42, no. 9, pp. 4004-35. Available from: https://doi.org/10.1039/C2CS35330J

[10] GROEN, J.C., PEFFER, L.A.A., MOULIJN, J.A., PÉREZ, R., X, REZ, J. On the introduction of intracrystalline mesoporosity in zeolites upon desilication in alkaline medium. *Microporous and Mesoporous Materials*. 2004, vol. 69, no. 1, pp. 29-34. Available from: https://doi.org/10.1016/j.micromeso.2004.01.002

[11] BRAVO, L.M., KOPYSCINSKI, J. Trade-offs in stability and activity: A study of ordered mesoporous alumina and γ-Al2O3 supported Ni catalysts for CO2 methanation. *The Canadian Journal of Chemical Engineering*. 2025, vol. 103, no. 12, pp. 6042-55. Available from: https://doi.org/10.1002/cjce.25755

[12] GROEN, J.C., BACH, T., ZIESE, U., DONK, A., DE JONG, K.P., MOULIJN, J.A., PÉREZ-RAMÍREZ, J. Creation of hollow zeolite architectures by controlled desilication of Al-zoned ZSM-5 crystals. *J Am Chem Soc*. 2005, vol. 127, no. 31, pp. 10792-3. Available from: https://doi.org/10.1021/ja052592x

[13] CORMA, A. From microporous to mesoporous molecular sieve materials and their use in catalysis. *Chemical Reviews*. 1997, vol. 97, no. 6, pp. 2373-419. Available from: https://doi.org/10.1021/cr960406n

[14] KARAM, L., BACARIZA, M.C., LOPES, J.M., HENRIQUES, C., REBOUL, J., HASSAN, N.E., MASSIANI, P. Mesoporous nickel-alumina catalysts derived from MIL-53(Al) metal-organic framework: A new promising path for synthesizing CO2 methanation catalysts. *Journal of CO2 Utilization*. 2021, vol. 51, pp. 101651. Available from: https://doi.org/10.1016/j.jcou.2021.101651

[15] ONRUBIA-CALVO, J.A., QUINDIMIL, A., DAVÓ-QUIÑONERO, A., BERMEJO-LÓPEZ, A., BAILÓN-GARCÍA, E., PEREDA-AYO, B., LOZANO-CASTELLÓ, D., GONZÁLEZ-MARCOS, J.A., BUENO-LÓPEZ, A., GONZÁLEZ-VELASCO, J.R. Kinetics, Model Discrimination, and Parameters Estimation of CO2 Methanation on Highly Active Ni/CeO2 Catalyst. *Industrial & Engineering Chemistry Research*. 2022, vol. 61, no. 29, pp. 10419-35. 10.1021/acs.iecr.2c00164